Fabrication of Ga₂O₃ thin films by aqueous solution deposition

Yutaka OHYA,[†] Jyunya OKANO, Yuki KASUYA and Takayuki BAN

Department of Materials Science and Technology, Faculty of Engineering, Gifu University, 1−1, Yanagido, Gifu 501−1193

Ga_2O_3 thin films were fabricated using the Ga nitrate and GaOOH aqueous solutions. The films were crystallized as β-Ga_2O_3 phase by heating at 700°C and the band gap of resultant films was about 4.9 eV. The films were uniform and the film from Ga nitrate solution was dense with porosity of about 3%. The resistivity of the blank film was about 10^7 Ω cm. The doped films with Ti and Zr exhibited rectifying properties on ITO sputtered glass substrate.

1. Introduction

Recently β-gallium oxide, β-Ga_2O_3, ceramic film has been extensively studied for its excellent opto-electronic properties. β-Ga_2O_3 is known as a nonstoichiometric n-type semiconductor with an adsorption edge of about 4.9 eV.[1)–3)] Since the electrical conductivity of the nonstoichiometric oxide depends on the formation of defects under equilibrium oxygen partial pressure, the fundamental defect chemistry over a wide range of oxygen partial pressure and their electrical conductivity have been studied.[4)–6)] The Ga_2O_3 semiconducting films are considered to be used as transparent conducting electrode for deep-UV applications,[2),7)] thin film transistors,[8)] gas sensing devices,[9)–12)] light emitting sources[13),14)] and so on.

The high conductive and transparent films were fabricated by the PLD method, and the conductivity of 1–8 S/cm was reported.[2),7)] The films were also fabricated by sputtering,[9),13),15)] MOCVD,[16)] sol–gel processes.[10)–13),17)] In order to control electrical or gas sensing properties, the tetravalent cations were attempted to be introduced into the lattice.[12)] The crystalline structure of β-Ga_2O_3 is very interesting to control oxide doping,[18)] since there are two kinds of polyhedron in the structure. There are apex-sharing tetrahedron arrays and edge-sharing octahedron arrays both along the b crystallographic direction. If doping of aliovalent cations can be done into the tetragonal site, the doping site can be separated from the conduction path, i.e., octahedron array, in the crystalline lattice.

The sol–gel processing for thin film preparation has advantages, i.e. easy preparation with low environmental emission and easy doping of aliovalent cations. Here, we report our results of the fabrication of Ga_2O_3 films from different starting aqueous sols. The aqueous precursors for Ga_2O_3 film were prepared from water soluble gallium nitrate and insoluble GaOOH. The GaOOH was examined, because so-called "alumina sol" was prepared by a peptization of AlOOH[19)] and the sol were used for Al_2O_3 film fabrication. Although the β-Ga_2O_3 film was already fabricated using the aqueous solution of Ga nitrate,[20)] the resultant film was composed of staking of the grains and the surface was not smooth. We tried to fabricate smooth and uniform film using the nitrate solution. The microstructure and electrical properties of cation doped films were also presented.

erties of cation doped films were also presented.

2. Experimental procedure

The reagents used were gallium nitrate hydrate ($Ga(NO_3)_3 \cdot 9H_2O$, 99.99% pure, Kojundo Chemical Laboratory Co., Ltd.) and gallium oxide hydroxide (GaOOH, 99.9% pure, Kojundo Chemical Laboratory Co., Ltd.). The nitrate is water soluble and we used the aqueous solution with addition of surfactant, 0.1 vol% of polyoxyethylene lauryl ether (Emulgen 108, Kao Chemicals), for fabrication of Ga_2O_3 thin film. Since gallium oxide hydroxide is insoluble in water, we tried some acids and tetramethylhydroxide (TMAOH) to make a clear solution. Among the tried chemicals of HCl, HNO_3, lactic acid, citric acid, acetic acid, and TMAOH, addition of 4 times molar of HCl and 3 times molar of TMAOH resulted in clear and transparent precursor solutions. Prior to coating experiments 0.4 mass% of polyacrylic acid (MW:250,000) was added into GaOOH solution peptized with HCl. Concentrations of prepared aqueous solutions were 0.5 M for gallium nitrate solution and 0.3 M for gallium oxide hydroxide solution.

After drying the solutions at 60°C, the dried matters were examined by thermogravimetry (TGA–50, Shimadzu Co.). Doping of tetravalent cations such as Si, Ti, Ge, Zr, and Sn was examined. The ionic radii of the cations after Shannon are listed in **Table 1**. In the Table the reagents used for the doping were also shown. The added amount of the dopants ranged from 1 to 5 mol% for Ga ion.

Table 1. Ionic Radius of Coordination Number (CN) of IV and VI in pm (after Shannon) and Reagents Used

Ion	CN		Reagent
	IV	VI	
Ga^{3+}	47	62	
Si^{4+}	26	40	Hydrolyzed TEOS by HCl
Ge^{4+}	39	53	Dissolved GeO_2 in nitric acid solution
Ti^{4+}	42	61	Titanium lactate from alkoxide and lactic acid
Sn^{4+}	55	69	Deflocculated stannic acid from $SnCl_4$
Zr^{4+}	59	72	Aqueous Zr acetate solution

† Corresponding author: Y. Ohya; E-mail: ohya@gifu-u.ac.jp

The solution was coated by dip-coating, i.e. after immersing a substrate into the solution, the substrate was withdrawn at a speed of 6 cm/min. The spin-on method was also used for coating the Ga nitrate solution by spinning speed of 3000 rpm for 30 s. The coated substrate was dried at 110°C for 10 min and then heated by inserting the film into a furnace maintained at a target temperature for 30 min. The substrate used was heat resistant glass (#1737, Corning) with and without sputtered transparent ITO electrode, and silica glass.

The crystalline phase of the resultant films was determined by XRD (RAD–2R, Rigaku Co.) and their microstructure was observed by FE–SEM (S–4300 and S–4800, Hitachi, Ltd.) and TEM (H–8100, Hitachi, Ltd.). Optical transmittance was measured by a spectrometer (U–4000, Hitachi, Ltd.) and porosity of the film was evaluated using an equation of Lorentz–Lorenz from the obtained refractive index.[21] Optical band-gap was also estimated from the spectrum. Electrical resistivity of the film was measured using a double-ring probe method of an ohmmeter (Hiresta-IP, Mitsubishi-Yuka) and an electrometer (Keithley, 6517A, USA).

3. Results and discussion

3.1 Preparation of aqueous solutions and coating

A clear and transparent solution could be obtained by an addition of HCl with 4-times molar of GaOOH followed by refluxing in N_2 atmosphere for 2 h. (Abbreviated as GaOOH–HCl solution) Since the solution exhibited very little Tyndall effect by He–Ne laser, the solution was not colloid solution but an acidic solution of gallium chloride. An addition of TMAOH with 3-times to GaOOH resulted in a clear and transparent solution with Tyndall effect. The results of TGA analysis of the dried matter of GaOOH–HCl solution and $Ga(NO_3)_3 \cdot 9H_2O$ were shown in **Fig. 1**. The mass loss of $Ga(NO_3)_3 \cdot 9H_2O$ at 800°C was almost the same as the change of the nitrate to the oxide. The dried matter of GaOOH–HCl solution exhibited gradual mass loss till 250°C and then 24% from 520 to 550°C. The mass loss of 24% was estimated as the change of $Ga(OH)_2Cl$ to Ga_2O_3, where the loss is about 22%.

The three kinds of prepared solution were coated on the glass substrate. Using the GaOOH–HCl and Ga nitrate solutions, oxide thin films of good quality were obtained by heating at 700°C. Based on the results, the Ga_2O_3 films were fabricated using GaOOH–HCl and Ga nitrate aqueous solutions.
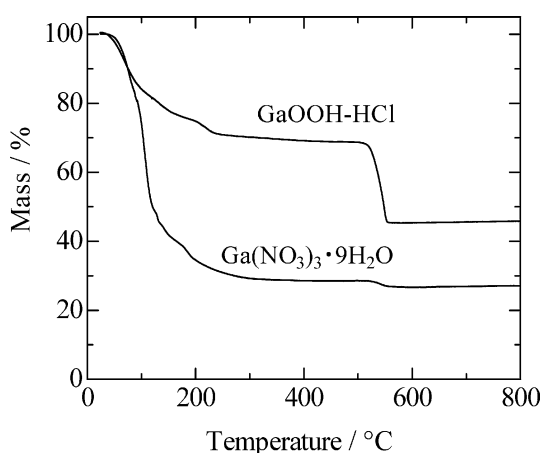
3.2 Crystallization and optical properties of Ga₂O₃ films

Since the decomposition of the GaOOH–HCl solution to Ga_2O_3 completed at about 550°C as shown in Fig. 1 and the film heated at 600°C didn't crystallize as Ga_2O_3 phase, the crystalline Ga_2O_3 film was obtained by heating at 700°C. The result of the XRD measurement of the film deposited by the dip-coating procedure with 10 times repetition GaOOH–HCl solution was shown in **Fig. 2**(a). In Fig. 2, β-Ga₂O₃ powder prepared by heating of GaOOH powder at 1050°C and peaks of monoclinic β-Ga₂O₃ of JCPDS #41–1103 were also shown. The XRD peaks of β-Ga₂O₃ film and powder were the same as the JCPDS data and the crystallization of monoclinic β phase by heating at 700°C was confirmed.

The transmission of UV-Vis region of the films fabricated by the dip-coating method from the solutions of GaOOH–HCl and Ga nitrate on the silica glass substrate were shown in **Fig. 3**. All the films were transparent and clear, and there were interference bands due to the uniform optical thickness (product of film thickness and refractive index). Although the adsorption edge of the samples was about 250 nm and coincident with the optical band gap of 4.8–4.9 eV, the existence of the interference bands prevented the accurate calculation of the band gap from the results of Fig. 3. The interference bands can be used for evaluation of refractive index and film thickness. The resultant thickness of the dip coating film from Ga nitrate solution was about 37 nm per single coating and this value was almost the same as the single coating thickness evaluated by SEM micrographs, which was 35 nm. This thickness of 35 nm was used for the calculation of resistivity in the following section. The single coating thickness of GaOOH–HCl was about 42 nm, though the concentration of GaOOH–HCl was 60% of Ga nitrate solution. This suggested that viscosity of the GaOOH–HCl solution was higher than the nitrate solution. The single coating thickness of the spin-on method using Ga nitrate solution was about 20 nm under the present conditions.

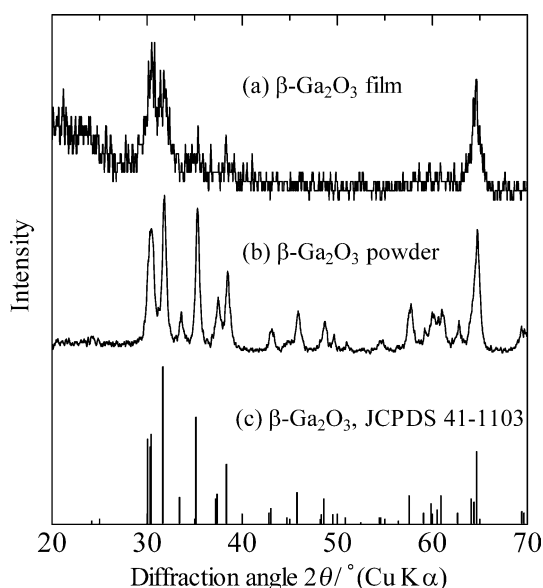The refractive index of the films (a), (b), and (c) in Fig. 3 were

Fig. 1. TGA thermograms of dried matters at 60°C of GaOOH–HCl and Ga nitrate aqueous solutions.

Fig. 2. XRD profiles, (a) Ga_2O_3 films from GaOOH–HCl solution heated at 700°C and deposited 10 times, (b) Ga_2O_3 powder prepared by heating of GaOOH powder at 1050°C and (c) β-Ga₂O₃ profile after JCPDS #41–1103.

1.84, 1.76 and 1.92 for the films from (a) Ga nitrate solution and dip-coating, (b) GaOOH–HCl solution by dip-coating, and (c) Ga nitrate solution of spin-on method, respectively. The film porosity could be estimated using these index values using a Lorentz–Lorent equation. If the refractive index of non-porous film was considered as 1.95,[22] the porosity of the film was calculated being 8, 15, and 3%, as the order of appearance above. The porous film form GaOOH–HCl solution is owing to the decomposition of $Ga(OH)_2Cl$ to Ga_2O_3 at about 550°C and the dense film of spin-on method was due to repetition of a thin coating. The relation of a single coating thickness and film density

Fig. 3. UV-Vis spectra of Ga_2O_3 films heated at 700°C on silica glass substrate and adsorption edge of the films.

was the same as that reported previously.[21]

The addition of the tetravalent dopants resulted in the clear and transparent films at 700°C, which were fabricated by the spin-on method on a heat resistance glass substrate with 5 times depositions. Tough films were crystallized as β-Ga_2O_3 phase after heating at 700°C, the XRD peak intensity was less than the blank film fabricated by the same conditions. Because of the low intensity of the XRD peaks, we could not determine changes in lattice constants and therefore formation of solid solution of doped β-Ga_2O_3 phase.

3.3 Microstructure of the films

The cross-sectional microstructure of Ga_2O_3 films fabricated by dip-coating method with 10 times repetitions was shown in **Figs. 4**(a), (b) and **Fig. 5**. As shown in Fig. 4, the films fabricated using Ga nitrate solution, Fig. 4(a), and GaOOH–HCl solution, Fig. 4(b), were uniform in thickness and the grain size of the former film seemed to be larger than the latter one. Both films seemed to be dense and this contradicted the estimation from the reflective index mentioned above. In order to examine this discrepancy, the film with 5 depositions using the GaOOH–HCl solution was fabricated and the last heating time was prolonged from 30 min to 2 h. The resultant film was shown in Fig. 4(c). The five layers corresponding to the deposition times are very clear and there are large void between the layers. This change in the microstructure means that very small pores in the film from GaOOH–HCl solution coalesced with each other to make large voids during long heating time and this film was porous.

TEM observation of the films of Figs. 4(a) and (b), shown in Fig. 5, revealed the structures in detail. Although both the films exhibited a layered structure and this is frequently observed among the films of solution deposition methods,[21] the film from GaOOH–HCl solution showed a very clear layered structure and the upper layers were separated. The lower layer of this film became dense and the grain grew larger, which indicated an occurrence of sintering during accumulated soaking time at 700°C by repetition of the coating-heating.

The discrete layered structure of the film from GaOOH–HCl solution was attributed to the high decomposition temperature, about 550°C, of $Ga(OH)_2Cl$ to Ga_2O_3 and the solution was not a
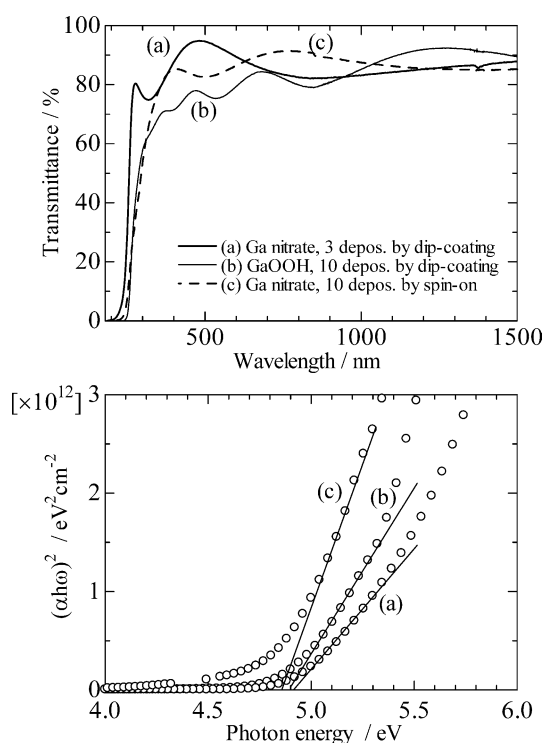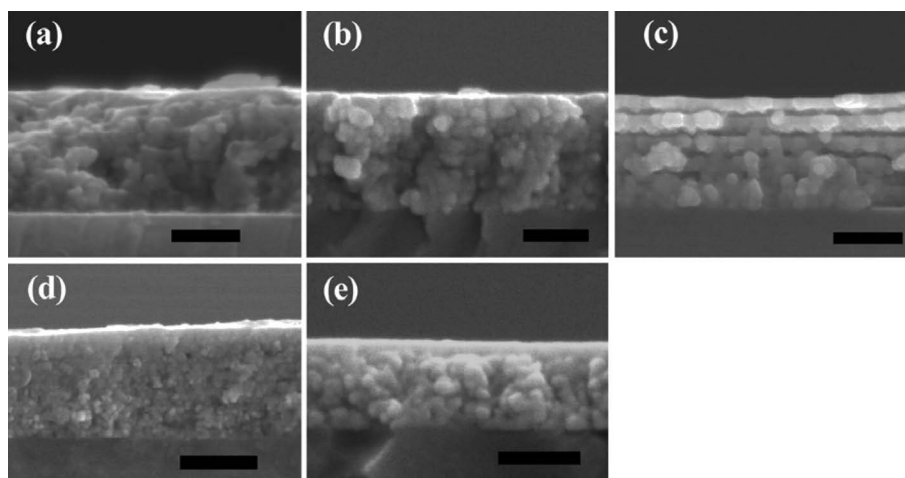

Fig. 4. SEM micrographs of Ga_2O_3 films heated at 700°C deposited by dip-coating method on #1737 glass substrate, (a) Ga nitrate solution deposited 10 times, bar: 200 nm, (b) GaOOH–HCl solution deposited 10 times, bar: 200 nm, (c) GaOOH–HCl solutions deposited 5 times with the last heating time prolonged to 2 h, bar: 150 nm, (d) Zr doped Ga nitrate solution deposited 10 times, bar: 500 nm and (e) Ti doped Ga nitrate solution deposited 5 times, bar: 200 nm.

suitable precursor for dense Ga$_2$O$_3$ film. Although this structure is favored for gas sensing devices, for example, the electrical conductive properties of the Ga$_2$O$_3$ film were examined using the solution of the Ga nitrate.

Microstructures of the films doped with Zr and Ti and fabricated by 10 and 5 times of dip coating depositions were also shown in Figs. 4(d) and (e), respectively. The single coating thickness of Zr and Ti doped films was about 70 and 42 nm, respectively. The addition of Zr acetate solution increased the single coating thickness, which suggested the increase in viscosity of the solution. The individual grain size of the two films was not so different and about 20–30 nm.

The films with dopants fabricated by the spin-on method with 5 times deposition exhibited uniform film thickness with a smooth surface. The grain size of the β-Ga$_2$O$_3$ phase was 20–30 nm and single coating thickness of the film was about 20 nm except the film doped with Zr. The addition of Zr acetate aqueous solution made the film of 33 nm thickness of single coating.
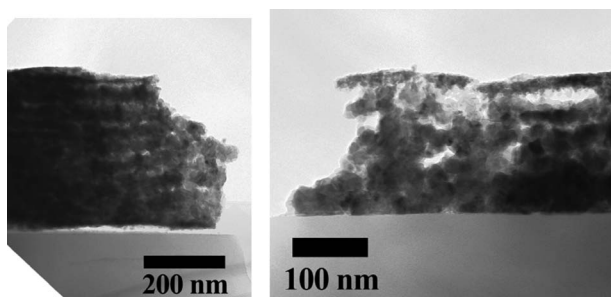

Fig. 5. TEM micrographs of Ga$_2$O$_3$ films heated at 700°C deposited by dip-coating method on #1737 glass substrate, (left) Ga nitrate solution deposited 10 times and (right) GaOOH–HCl solution deposited 10 times.

3.4 Electrical resistivity of the Ga$_2$O$_3$ film

The blank and doped films for evaluation of electrical resistivity were fabricated by the spin-on method of 5 times depositions, because the film by spin-on method became dense as described above. The resistivity of the films was examined by the double-ring probe. The resultant resistivity ranged from 10^4 to 10^7 Ω cm, which was independent on the kind and amount of dopants of 1 to 5%. This means the accurate measurement of the resistivity is difficult, because the films had very high resistance and surface conduction of the film affected the resistivity. In addition the resistivity of the film increased gradually during storage in a desiccator. Typically the resistivity of the blank film increased from 2×10^6 Ω cm just after the fabrication to 6×10^7 Ω cm for 800 h duration in the desiccator. One of the possible reasons of the change in the resistivity of the films was an adsorption of negatively charged oxygen from the air, which formed a high resistive space charge layer on the surface.

In order to minimize the effect of surface conduction, resistivity along the direction of thickness was measured. The Ga$_2$O$_3$ films were deposited by the dip-coating method on the glass substrate (#1737, Corning) sputtered with ITO transparent electrode. The Ga nitrate solution doped with 5 mol% germanium, titanium, or zirconium and a blank one was coated 5 times and heated at 700°C for 30 min. After the deposition of gold electrode of 1.54 mm^2 on the Ga$_2$O$_3$ film, the I–V characters were measured and they were shown in **Fig. 6**. The blank film of 175 nm thick, shown as Fig. 6(a) exhibited a linear voltage-current relation and the resistivity of the film was calculated being 1.6×10^7 Ω cm. The resistance of the germanium doped sample, which was not shown in the Fig. 6, was almost the same order of magnitude as the ITO electrodes and cracks and/or pores on the film acted as leakage paths of the current.

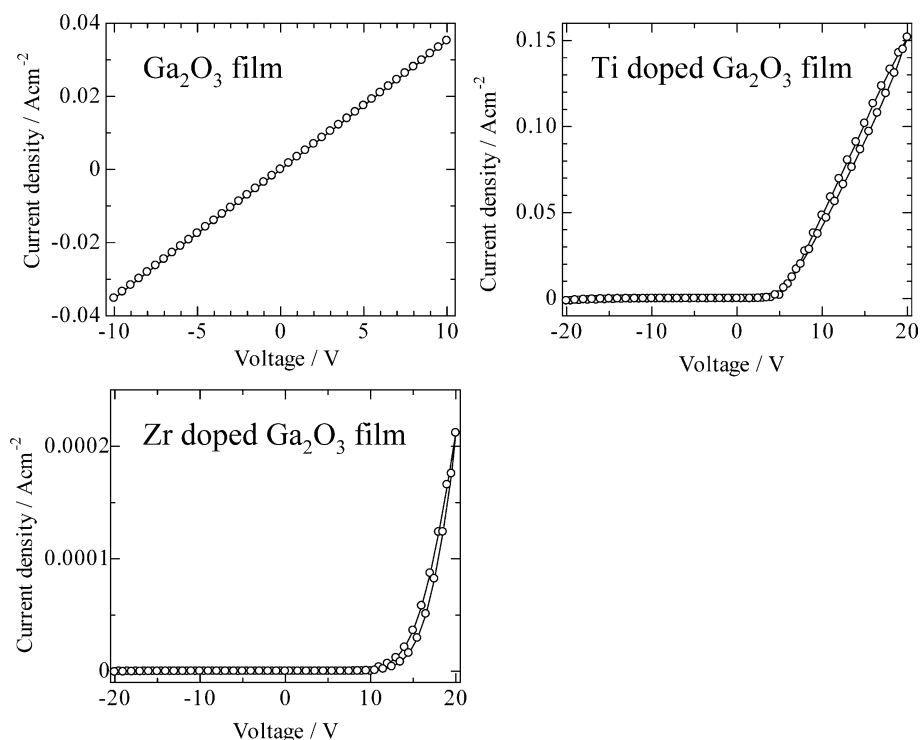The titanium and zirconium doped films exhibited the non-

Fig. 6. I–V characteristics of Au–Ga$_2$O$_3$–ITO/glass samples doped with 5% of Ti and Zr. The films were fabricated using Ga nitrate solution by 5 times deposition of dip-coating method heated at 700°C.

linear I–V characteristics as shown in Fig. 6(b) and (c), respectively. The thicknesses of the film were 210 and 350 nm, respectively. The current increased rapidly on the ITO electrode being a positive bias and showed rectifying properties. This seemed to be a metal-semiconductor Schottky effect, which was caused by the interface between the ITO and Ga_2O_3 interface and not the Au and Ga_2O_3 interface.[23]

The Ga_2O_3 film is utilized as gas sensing devices using the Schottky diode properties and the Schottky barrier was formed between the contact with Pt electrode.[10),11)] The electrical properties of Ga_2O_3 nanowire also revealed that the contact of Ga_2O_3 with Pt electrode formed Schottoky barrier and the current through Pt–Ga_2O_3–Pt configuration was nonlinear, while the ohmic contact was formed by a contact with Ti.[24] In the case of n-type semiconductors, such as Ga_2O_3, the Schottky barrier was formed when the semiconductor contacted with the metal having a larger work function than that of the semiconductor. Although ITO is known as an electrode with a large work function of 4.55 eV,[25] the value is almost the same as that of Ti, 4.33 eV. A work function of another electrode, Au, is almost the same as Pt, about 5.4 eV for Au and about 5.6 eV for Pt. Based on the simple concept of forming the Schottky effect, present non-linear and rectifying I–V character of Ti and Zr doped Ga_2O_3 films was opposite to the usual Schottky barrier. Further, the cut-on voltages were about 5 and 12 V for doped films with titanium and zirconium, respectively. The voltages are very large comparing the usual Schottky diode and a transport mechanism of electron through the barrier, though the cut-on voltage of Pt–Ga_2O_3 nanowire-Pt configuration was about 5 V.[24] The current density of Ti doped film for forward bias was about 1000 times larger than that of Zr doped film and the two films examined were very different in their carrier transport mechanism. In order to solve the present non-linear I–V character of doped films, characterization of both the Ga_2O_3 and the interface was inevitable, which is now in progress.

4. Conclusion

The Ga_2O_3 film was fabricated via aqueous solution deposition method. The Ga nitrate and GaOOH–HCl solutions were used for fabrication with the addition of surfactant and polymer, and the resultant films were very uniform in optical thickness. The films crystallized as β-Ga_2O_3 phase by heating at 700°C. The film from GaOOH–HCl was very porous and had a layered structure because of the high decomposition temperature of $Ga(OH)_2Cl$ to Ga_2O_3. The film from Ga nitrate solution was dense with estimated porosity of about 3%. The band gap of the films was about 4.9 eV and the same as the published data. Resistivity of the blank film was about 10^7 Ω cm and doping of tetravalent cations hardly decreased the resistivity under the present conditions. The films doped with Ti and Zr exhibited the non-linear and rectifying I–V characteristics between the Ga_2O_3 film and ITO electrode interface. The reason of the rectifying character was not realized.

Reference

1) M. Passlack, E. F. Schubert, W. S. Hobson, M. Hong, N. Moriya, S. N. G. Chu, K. Konstadinidis, J. P. Mannaerts, M. L. Schnoes and G. J. Zydzik, *J. Appl. Physics*, **77**, 686–693 (1995).
2) M. Orita, H. Ohta, M. Hirano and H. Hosono, *Appl. Phys. Lett.*, **77**, 4166–4168 (2000).
3) M. Rebien, W. Henrion, M. Hong, J. P. Mannaerts and M. Fleischer, *Appl. Phys. Lett.*, **81**, 250–252 (2002).
4) M. Fleisher, L. Hoellbauer, E. Born and H. Meixner, *J. Am. Ceram. Soc.*, **80**, 2121–2125 (1997).
5) A. Feltz and E. Gamsjaeger, *J. Eur. Ceram. Soc.*, **18**, 2217–2226 (1998).
6) M. Zinkevich and F. Aldinger, *J. Am. Ceram. Soc.*, **87**, 683–691 (2004).
7) M. Orita, H. Hiramatsu, H. Ohta, M. Hirano and H. Hosono, *Thin Solid Films*, **411**, 134–139 (2002).
8) M. Matsuzaki, H. Hiramatsu, K. Nomura, H. Yanagi, T. Kamiya, M. Hirano and H. Hosono, *Thin Solid Films*, **496**, 37–41 (2006).
9) M. Fleischer and H. Meixner, *Sens. Actuators B*, **4**, 437–441 (1991).
10) A. Trinchi, W. Wlodarski and Y. X. Li, *Sens. Actuators B*, **100**, 94–98 (2004).
11) A. Trinchi, S. Kaciulis, L. Pandolfi, M. K. Ghantasala, Y. X. Li, W. Wlodarski, S. Viticoli, E. Comini and G. Sberveglieri, *Sens. Actuators B*, **103**, 129–135 (2004).
12) Y. Li, A. Trinchi, W. Wlodarski, K. Galatsis and K. Kalantar-Zadeh, *Sens. Actuators B*, **93**, 431–434 (2003).
13) T. Miyata, T. Nakatani and T. Minami, *Thin Solid Films*, **373**, 145–149 (2000).
14) S. Fujihara and Y. Shibata, *J. Lumin.*, **121**, 470–474 (2006).
15) A. Bausewein, B. Hacker, M. Fleischer and H. Meixner, *J. Am. Ceram. Soc.*, **80**, 317–323 (1997).
16) H. W. Kim and N. H. Kim, *J. Alloys Compd.*, **389**, 177–181 (2005).
17) G. Sinha, K. Adhikary and S. Chaudhuri, *Opt. Mater.*, **29**, 718–722 (2007).
18) J. Åhman, G. Sevensson and J. Albertsson, *Acta Cryat.*, **C52**, 1336–1338 (1996).
19) B. E. Yoldas, *Am. Ceram. Soc. Bull.*, **54**, 289–290 (1975).
20) S. Fujihara, Y. Shibata and E. Hosono, *J. Electrochem. Soc.*, **152**, C764–C768 (2005).
21) Y. Ohya, H. Saiki, T. Tanaka and Y. Takahashi, *J. Am. Ceram. Soc.*, **79**, 825–830 (1996).
22) "CRC Handbook of Chemistry and Physics," Ed. by R. C. Weast (1989) p. B-92.
23) K. F. Brennan, "The Physics of Semiconductors," Cambridge Univ. Press (1999) pp. 589–597.
24) Y. Huang, S. Yue, Z. Wang, Q. Wang, C. Shi, Z. Xu, X. D. Bai, C. Tang and C. Gu, *J. Phys. Chem. B*, **110**, 796–800 (2006).
25) M. M. Beerbom, B. Laegel, A. J. Cascio, B. V. Doran and R. Schlaf, *J. Electron Spectrosc, Relat. Phenom.*, **152**, 12–17 (2006).